Acta Cryst. (1982). B**38**, 2626–2632

Experimental and Theoretical Difference Densities for Thiourea. Refinement of Electron Density Distributions with Charge-Cloud Models. X.* Comparison of Observed and Calculated Electron Densities. XIII†

BY ALI KUTOGLU AND CHRISTIAN SCHERINGER

Institut für Mineralogie der Universität Marburg, D-3550 Marburg/Lahn, Federal Republic of Germany

AND HERMANN MEYER AND ARMIN SCHWEIG

Fachbereich Physikalische Chemie der Philipps-Universität, Hans-Meerwein-Strasse, D-3550 Marburg, Federal Republic of Germany

(*Received* 27 *March* 1981; *accepted* 23 *September* 1981)

Abstract

Because of the large deviations of the experimental deformation density from a corresponding theoretical density, the X-ray data for thiourea at 123 K [Mullen & Hellner (1978). *Acta Cryst.* B**34**, 2789–2794] have been reinspected. It was found that the background measurements were erroneous on one side and they have been reprocessed. Refinement with the conventional free-atom model yielded $R(F) = 0{\cdot}0184$ for 1099 (observed) data. X–X(high-angle parameter) maps are presented with the phases for the F_o's taken from the free-atom model and from a charge-cloud model of the density distribution. The refinement with the charge-cloud model is described and yielded $R(F) = 0{\cdot}0125$. Dynamic and static deformation densities calculated from the charge-cloud model are presented. The two (half) molecules in the asymmetric unit have unequal density distributions in the C–S regions. A theoretical (4-31G + BP) calculation of the static and dynamic deformation densities is presented. The agreement between theoretical and experimental dynamic deformation densities is very good for one molecule, the maximum deviation between the peak heights being 0·05 e Å^{-3}. For the other molecule, the agreement is as good except for the C–S bond region where the experimental deformation density is lower by 0·25 e Å^{-3}.

Introduction

X-ray data on thiourea at 123 K were collected by Mullen & Hellner (1978). Deformation densities based on these data exhibited peaks and troughs at the S atom that were much too pronounced (Mullen & Scheringer, 1978; and unpublished work) when compared to corresponding theoretical densities (H. Meyer & A. Schweig, unpublished work; now presented below).

A recent inspection of the original diffractometer output showed, on the one hand, that the measured intensities were not corrected for anomalous scattering at the S atom and, on the other hand, that, with about 40% of the reflections, the background at one side was measured as being much too large. Furthermore, the extinction correction applied by Mullen & Hellner (1978) was probably insufficient. Since the data still appeared to be of high quality [Mullen & Hellner obtained $R(F) = 0{\cdot}025$ with the free-atom model and 1142 data], we have reprocessed the original diffractometer output of Mullen & Hellner (1978).

We first describe some items of our data reduction and the refinements with the conventional free-atom model. Then we present X–X(high-angle parameter) maps which we shall use as a basis for the concept of a charge-cloud model of the density distribution in the molecule. Finally, we describe the refinement with the charge-cloud model and present dynamic and static deformation densities calculated from this model.

In the second part of this paper, the results of the theoretical calculation of the electron density distribution in the thiourea molecule (mentioned above) will be presented and compared with the experimental densities.

Treatment of the data

We have corrected Mullen & Hellner's (1978) diffractometer output for the errors in the background measurements, for anomalous scattering of the S atom and for (isotropic) extinction. With $\mu = 0{\cdot}629$ mm^{-1}

* The title of the series has been changed. The previous title was 'A Simple Refinement of Density Distributions of Bonding Electrons'.

† Part XII: Fuess, Bats, Dannöhl, Meyer & Schweig (1982).

0567-7408/82/102626-07$01.00

and a radius of $r = 0.25$ mm for the spherically ground crystal, the absorption factor is constant over the whole region of measurement ($A = 1.31$) and, hence, an absorption correction is superfluous. The largest effect on the improvement of the data was the correction of the background; the extinction correction was also important, whereas the effect of the correction for anomalous scattering was nearly negligible. We still give here some results for this correction, since they are probably typical for molecular crystals in which the S atom contributes only in part to the total scattering. Thus we hope to help other workers to judge a corresponding situation more easily.

With anomalous scattering of the S atom, the intensities of the reflections hkl, $h\bar{k}l$ (class 1) and $\bar{h}kl$, $\bar{h}\bar{k}l$ (class 2) are different in the space group $P2_1ma$. We have reduced them separately and have performed the averaging over the two classes only with the F_o's and $\sigma(F_o)$'s. The relevance of the correction for anomalous scattering at thiourea may be seen from a statistic given in Table 1. In order to assess the differences of intensity in the two classes and to compare them with the theoretical expectation, we have calculated inter-class R values (see also Table 1). These figures show that, on the average over the several groups of reflections and over all reflections, the experimental accuracy is not high enough to allow us to distinguish between the systematic differences of the intensities in the two classes. This also holds for those groups of reflections which are most affected by anomalous scattering (groups 5 and 6 in Table 1). However, the systematic nature of the effect of anomalous scattering at the S atom can be seen more clearly in the deformation densities (not given here) calculated with both sets of experimental structure factors (the F_{exp}'s and the F_o's). These deformation densities differ by 0.07 e Å^{-3} at the S atom, whereas in the remaining molecule the differences are at most 0.03 e Å^{-3}.

Table 1. *Effects of anomalous scattering of the* S *atom* ($f' = 0.110$, $f'' = 0.124$, *International Tables*) *on the structure factors of thiourea*

$|F_c^*|$: structure factor calculated with f' and f'' for the S atom
$D = |F_c|/|F_c^*|$, $R_{AS} = 2\sum||F_c| - |F_c^*||/\sum(|F_c| + |F_c^*|)$
Inter-class R values: $R_{12} = 2\sum|F_1 - F_2|/\sum(F_1 + F_2)$
R_{12}^{exp}: value for the experimental F_{exp}'s (not corrected for anomalous scattering)
R_{12}^{obs}: value for the experimental F_o's
R_{12}^{th}: value for the calculated $|F_c^*|$'s

The R_{AS} values are the same for the two classes, with the number of digits given. For the two classes, only a few reflections do not fall into the same $|1 - D|$ groups. $|1 - D|$ and the R values are given in per cent.

$\|1-D\|$	Number of reflections class 1	class 2	R_{AS}	R_{12}^{exp}	R_{12}^{obs}	R_{12}^{th}
0–1	274	275	0.6	1.26	1.19	0.52
1–2	439	438	1.5	1.11	1.09	0.47
2–3	273	271	2.4	1.53	1.53	0.76
3–4	76	79	3.4	2.80	2.36	0.90
4–5	27	28	4.6	5.02	5.11	1.29
>5	53	51	8.7	11.75	10.73	2.03
–	1142	1142	1.5	1.33	1.33	0.56

The corrections for the background measurements were performed as follows: We formed groups of 10–90 reflections dependent on sin θ/λ, and represented the average background in each group graphically as a function of sin θ/λ. For the background at side 1 we found a weakly decreasing straight line, to a good approximation. The background at side 2 showed in the region $0.2 \le \sin\theta/\lambda \le 0.65$ Å^{-1}, *i.e.* for 40% of all reflections, an irregularly formed elevation with peak values being 21 times larger than the background at side 1. In the remaining regions of sin θ/λ the background for the two sides was largely equal. In the reduction of the data we have then used the averaged background at side 1.

The region of measurement extended up to sin $\theta/\lambda = 0.9$ Å^{-1} with 1142 independent reflections. After background correction and after averaging over the symmetry-equivalent reflections within the classes, we obtained for class 1 from 2184 measured intensities $R_i(I) = 0.0351$, $R_i(F^2) = 0.0299$, $R_i(F) = 0.0156$, and for class 2 from 2182 measured intensities $R_i(I) = 0.0453$, $R_i(F^2) = 0.0454$, $R_i(F) = 0.0255$.* 43 reflections were classified as *unobserved*, with $I < 2\sigma(I)$.

Refinements with the conventional free-atom model

This model was refined with the 1099 observed data and then with the 683 high-angle data, with sin $\theta/\lambda \ge 0.65$ Å^{-1}. For the H atoms Elcombe & Taylor's (1968) neutron parameters were used and kept constant. Weights were taken as $w = 1/\sigma^2(F_o)$. With 1 scale factor and 41 positional and thermal parameters of the C, N and S atoms, we obtained with the full-angle data $R(F) = 0.0184$, $R_w(F) = 0.0274$, GoF = 0.62, and for the scale factor $K = 1.00418$. With this scale factor and the 683 high-angle data, we obtained $R(F) = 0.0153$, $R_w(F) = 0.0230$, GoF = 0.41. The parameters are given in Table 2, and the bond lengths in Table 3.

For the various sets of thermal parameters we have calculated Hirshfeld's (1976) rigid-bond test (Table 4). According to the rigid-bond postulate one would expect to find ΔU(bond direction) ≤ 0.0010 Å^2, and for bonds involving H ΔU(bond direction) ≤ 0.0050 Å^2 (because of the larger amplitudes of the H atoms in the stretching modes). The test shows the worst results for

*$R_i(I) = \sum$ refl. $\sum_{k=1}^{s}|I_k - \bar{I}|/\sum$ refl. $S\bar{I}$; $\bar{I} = S^{-1}\sum_{k=1}^{s} I_k$, S = number of symmetry-equivalent members per reflection.

Elcombe & Taylor's (1968) neutron parameters (row *d* in Table 4). We still used Elcombe & Taylor's parameters for the H atoms because we believed that we would not be able to determine better parameters from the X-ray data. The best test values are shown by our high-angle parameters (row *b*); on the whole, they

Table 2. *Positional and thermal parameters for thiourea at* 123K

(i) Positional parameters in lattice units

		x	*y*	*z*			*x*	*y*	*z*
Molecule (1)					Molecule (2)				
S(1)	(*a*)	0·0052 (2)	0	0·3458 (1)	S(2)	(*a*)	0·0248 (2)	0·5	0·1230 (1)
	(*b*)	0·0053 (2)	0	0·3457 (1)		(*b*)	0·0249 (2)	0.5	0·1230 (1)
	(*c*)	0·0051 (2)	0	0·3458 (1)		(*c*)	0·0247 (1)	0·5	0·1230 (1)
	(*d*)	0·0062 (16)	0	0·3454 (19)		(*d*)	0·0272 (16)	0·5	0·1215 (7)
C(1)	(*a*)	0·0736 (3)	0	0·0470 (2)	C(2)	(*a*)	−0·0981 (3)	0·5	0·3866 (3)
	(*b*)	0·0734 (3)	0	0·0467 (2)		(*b*)	−0·0982 (3)	0·5	0·3867 (3)
	(*c*)	0·0735 (2)	0	0·0467 (2)		(*c*)	−0·0982 (2)	0·5	0·3867 (2)
	(*d*)	0·0733 (10)	0	0·0455 (7)		(*d*)	−0·0985 (9)	0·5	0·3860 (6)
N(1)	(*a*)	0·1	0·1336 (1)	−0·0739 (2)	N(2)	(*a*)	−0·1476 (2)	0·3660 (1)	0·4921 (2)
	(*b*)	0·1	0·1339 (1)	−0·0741 (2)		(*b*)	−0·1476 (2)	0·3659 (1)	0·4920 (2)
	(*c*)	0·1	0·1338 (1)	−0·0737 (1)		(*c*)	−0·1477 (2)	0·3658 (1)	0·4922 (2)
	(*d*)	0·1	0·1337 (3)	−0·0756 (4)		(*d*)	−0·1475 (5)	0·3656 (3)	0·4912 (6)

(ii) Thermal parameters ($\beta_{ij} \times 10^4$). The components β_{ij} refer to the form $\exp[-(\beta_{11}h^2 + \ldots 2\beta_{12}hk + \ldots)]$.

		11	22	33	12	13	23			11	22	33	12	13	23
Molecule (1)								Molecule (2)							
S(1)	(*a*)	92 (1)	44 (1)	74 (1)	0	3 (1)	0	S(2)	(*a*)	76 (1)	39 (1)	91 (1)	0	5 (1)	0
	(*b*)	92 (1)	44 (1)	73 (1)	0	3 (1)	0		(*b*)	76 (1)	39 (1)	91 (1)	0	5 (1)	0
	(*c*)	91 (1)	44 (1)	73 (1)	0	3 (1)	0		(*c*)	76 (1)	39 (1)	90 (1)	0	5 (1)	0
	(*d*)	99 (21)	26 (12)	52 (30)	0	−20 (19)	0		(*d*)	86 (17)	35 (12)	34 (27)	0	−14 (8)	0
C(1)	(*a*)	66 (2)	42 (1)	96 (3)	0	12 (2)	0	C(2)	(*a*)	55 (2)	42 (1)	112 (3)	0	2 (2)	0
	(*b*)	70 (1)	41 (1)	91 (2)	0	14 (1)	0		(*b*)	57 (1)	40 (1)	111 (2)	0	3 (1)	0
	(*c*)	69 (1)	42 (1)	93 (2)	0	13 (1)	0		(*c*)	56 (1)	40 (1)	110 (2)	0	3 (1)	0
	(*d*)	73 (10)	19 (5)	54 (13)	0	6 (8)	0		(*d*)	51 (7)	49 (7)	61 (13)	0	9 (9)	0
N(1)	(*a*)	125 (2)	43 (1)	116 (2)	−1 (1)	42 (2)	5 (1)	N(2)	(*a*)	94 (1)	40 (1)	160 (2)	−1 (1)	44 (2)	6 (1)
	(*b*)	127 (2)	43 (1)	113 (2)	−2 (1)	42 (1)	5 (1)		(*b*)	96 (1)	39 (1)	161 (2)	−1 (1)	46 (1)	5 (1)
	(*c*)	128 (1)	42 (1)	113 (1)	−1 (1)	44 (1)	6 (1)		(*c*)	95 (1)	39 (1)	161 (2)	−1 (1)	46 (1)	6 (1)
	(*d*)	113 (4)	36 (4)	94 (8)	1 (5)	33 (7)	5 (5)		(*d*)	84 (4)	40 (4)	117 (8)	−9 (5)	37 (5)	3 (5)

(*a*) Free-atom model, full-angle data. (*b*) Free-atom model, high-angle data. (*c*) Molecular charge-cloud model. (*d*) Neutron diffraction parameters of Elcombe & Taylor (1968).

Table 3. *Bond lengths* (Å) *in thiourea at* 123 K

Models (*a*), (*b*), (*c*), (*d*) are as in Table 2. H positions are fixed at the neutron diffraction values of Elcombe & Taylor (1968).

Model	C(1)–S(1)	C(2)–S(2)	C(1)–N(1)	C(2)–N(2)	N(1)–H(1)	N(1)–H(2)	N(2)–H(3)	N(2)–H(4)
(*a*)	1·715 (1)	1·712 (1)	1·334 (1)	1·335 (1)	1·007 (4)	1·001 (4)	1·010 (5)	1·018 (5)
(*b*)	1·714 (1)	1·713 (1)	1·335 (1)	1·334 (1)	1·004 (4)	1·002 (4)	1·012 (5)	1·017 (5)
(*c*)	1·715 (1)	1·712 (1)	1·334 (1)	1·335 (1)	1·006 (4)	1·002 (4)	1·010 (5)	1·017 (5)
(*d*)	1·723 (11)	1·733 (11)	1·334 (3)	1·335 (4)	1·000 (8)	1·006 (8)	1·021 (8)	1·012 (10)

Table 4. *Rigid-bond test for the thermal parameters in thiourea*

The table contains the absolute values of the differences of the vibration components of the two respective atoms in the direction of the bond in $Å^2 \times 10^4$. Vibration tensors of the H atoms are fixed to the neutron diffraction values of Elcombe & Taylor (1968). Models (*a*), (*b*), (*c*), and (*d*) are as in Tables 2 and 3.

Model	C(1)–S(1)	C(1)–N(1)	C(2)–S(2)	C(2)–N(2)	N(1)–H(1)	N(1)–H(2)	N(2)–H(3)	N(2)–H(4)
(*a*)	13	8	13	16	19	13	41	128
(*b*)	6	5	10	12	23	15	40	132
(*c*)	10	12	10	14	24	16	39	130
(*d*)	34	46	44	34	42	41	2	124

follow the rigid-bond postulate well. The values for the full-angle parameters (row *a*) are markedly worse. The poor values of 0·0128–0·0132 Å^2 for the N(2)–H(4) bond with all our X-ray parameter sets are evidently caused by the use of Elcombe & Taylor's (1968) vibration tensor for H(4) which had probably been determined incorrectly.

X–X (high-angle parameter) maps

X–X maps, *i.e.* deformation densities of the type $\Delta\rho = K^{-1}\rho_o - \rho_c$(free-atom model) were calculated with the F_o's and the high-angle parameters (row *b* in Table 2). Firstly, the F_o's were given the phases which are obtained from the free-atom model. Fig. 1 shows clearly the bond peaks and the lone-pair peaks at the S atom. The most remarkable difference in the deformation density for the two molecules is for molecule (2) (Fig. 1*b*); only a small C–S bond peak of 0·06 e Å^{-3} is found (not drawn in Fig. 1*b*), whereas for molecule (1) (Fig. 1*a*) the C–S peak appears to have a normal height (0·26 e Å^{-3}).

Since the phases which are obtained from the free-atom model are known to be inaccurate for noncentrosymmetric structures (Mullen & Scheringer, 1978), we have used the phases from the charge-cloud model of the density distribution (see below) and calculated the *X–X* maps again (Fig. 2). The better phases for the F_o's lead to a considerable increase (0·2 e Å^{-3}) of the bond peaks; this is most in the N–H bonds of both molecules and in the C–S bond of molecule (1). On the other hand, the already flat lone-pair peaks at the S atoms are not increased. The deformation densities with the better phases (Fig. 2) agree better with the theoretical densities than those calculated with the phases from the free-atom model (Fig. 1) (see below, Fig. 6*b*).

In order to make visible the effect of the erroneous background measurements on the density distribution, we have calculated a further *X–X* map, with Mullen & Hellner's (1978) data (Fig. 3). The calculations were performed exactly as for Fig. 1: full-angle data refinement with inclusion of an isotropic-extinction parameter [$R(F)$ = 0·0245], determination of the high-angle parameters, and Fourier synthesis with phases from the free-atom model. Fig. 3 shows the same basic features as Fig. 1 but gives the impression of a higher noise level. There are more peaks and troughs outside the molecule where zero density is expected. The C–S bond peak in Fig. 3 is abnormally high (0·44 e Å^{-3}) for molecule (1) (with better phases it would probably increase to about 0·65 e Å^{-3}). For molecule (2), the peak does not lie on the line through C and S; because of the symmetry *m* it now appears as a double peak. The lone-pair peaks appear to be too high for both molecules (0·34 and 0·36 e Å^{-3}).

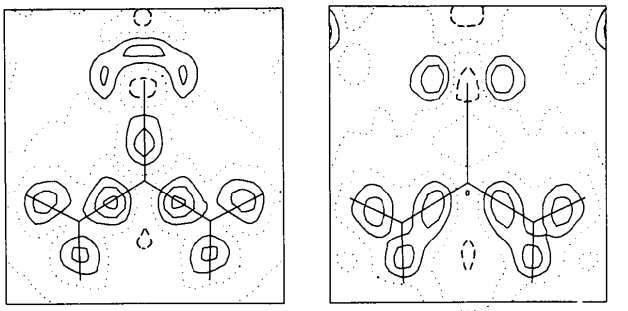

(*a*) (*b*)

Fig. 1. *X–X*(high-angle parameter) maps in the plane of the molecule. Phases for the observed structure factors are calculated from the free-atom model. Contour interval: 0·1 e Å^{-3}. Positive density: full lines; zero density: dotted; negative density: dashed. (*a*) Molecule (1), (*b*) molecule (2).

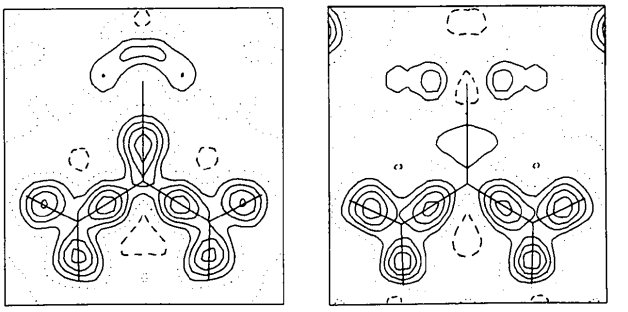

(*a*) (*b*)

Fig. 2. As Fig. 1, but with phases from the charge-cloud model.

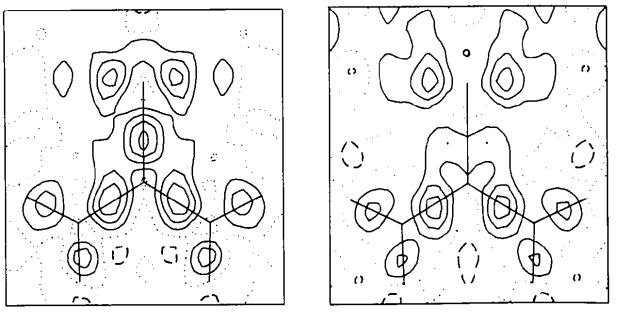

(*a*) (*b*)

Fig. 3. As Fig. 1, but with the original data of Mullen & Hellner (1978).

Refinements with the charge-cloud model

The type of model used was described by Dietrich & Scheringer (1978) and by Scheringer (1980). Gaussian-distributed negative charges are placed into the bond and lone-pair regions and spherically symmetric valence shells are correspondingly occupied by (mostly) positive charges. For each half molecule (with five atoms) we employed five charge clouds and five valence-shell charges. Each charge cloud has at most seven parameters (three positional parameters, three principal components of a smearing tensor referred to

the bond direction or other directions of molecular symmetry, one charge parameter). With the site symmetry m of the molecules, we thus obtain at most 78 density parameters. Electrical neutrality for each molecule reduces this number by 2. As shown by the X–X maps (Figs. 1 and 2), the molecules hardly differ in the regions of the C, N and H atoms, but in the regions of the C–S bonds they do differ. Thus, all density parameters referring to the C, N and H regions were set equal for the two molecules. Furthermore, the parameters for the bonds N–H(1) and N–H(2) within each molecule were also constrained to be equal, and rotational symmetry was introduced for all N–H bonds. In this way, the number of density parameters could be reduced to 35. For the 41 positional and thermal parameters, we first used the values obtained in the refinement with high-angle data, but finally also refined these parameters [except the parameters of the H atoms which were fixed to the values of Elcombe & Taylor (1978)]. With the 1099 observed data we obtained $R(F) = 0{\cdot}0125$, $R_w(F) = 0{\cdot}0179$ and GoF = 0·41.* The decrease of R and R_w relative to the corresponding values obtained with the free-atom model is highly significant, and is well below the tabulated value for $\alpha = 0{\cdot}005$ (*International Tables for X-ray Crystallography*, 1974). The final $F_o - F_c$ map shows residuals within $\pm 0{\cdot}1$ e Å^{-3}, except behind the S atom of molecule (1). The statistical error in the $F_o - F_c$ map, at some distance from the nuclei, is calculated to be $\sigma(\Delta\rho) = 0{\cdot}062$ e Å^{-3} (Rees, 1977). The scale factor now obtained is 1·00006. Parameters, bond lengths and rigid-bond-test values are given in Tables 2, 3 and 4 respectively. The density parameters are not given in detail, since the formation of the total distribution is possible in several ways, and the charges actually obtained depend much on the extension of the clouds. Similarly, the charges in the valence shells depend on the special formation of the remaining model and thus cannot be taken absolutely. We note that the charges in the clouds were found to range from 0·24 to 0·52 e, and the charges in the valence shells from 0·13 to 0·90 positive charge units (relative to the neutral atoms).

In order to investigate further the most conspicuous phenomenon of this structure, the different density distributions in the C–S bonds of the two molecules, we have calculated a further refinement in which the parameters referring to the C–S bonds were set to be equal (equal-molecule constraint with 24 density parameters). In both refinements, we used the high-angle parameters and kept them constant. The results were interpreted by means of Hamilton's (1965) R_w test. The reliability indices obtained are $R(F) = 0{\cdot}0141$, $R_w(F) = 0{\cdot}0185$, GoF = 0·418 for different densities in the C–S bonds, and $R(F) = 0{\cdot}0141$, $R_w(F) = 0{\cdot}0192$, GoF = 0·432 for equal densities. The number of parameters differ by 12. With the ratio 1·038 for the R_w values and with the theoretical value of 1·014 for $\alpha = 0{\cdot}005$ (*International Tables*), the hypothesis that the densities in the C–S bonds are equal can be rejected even far beyond the significance level of $\alpha = 0{\cdot}005$.

The possibility that the two different C–S bond peaks are due to incorrect vibration tensors of the S atoms could be excluded in the following way. We have changed the components in the directions of the C–S bonds by $\pm 0{\cdot}0005$ and $\pm 0{\cdot}0010$ Å^2, and perpendicular to these directions by the same amounts but with opposite sign, and have calculated the X–X maps again. We found changes of the density in a sphere of about 0·5 Å around the nuclear positions of the S atoms, but the C–S bond peaks were hardly affected. Furthermore, an inspection of the observed and calculated structure factors and Fourier syntheses with eliminated sets of F_o's showed that the contributions to the C–S bond densities and to the lone-pair regions of the S atoms do not arise from a particular group of reflections which might have been measured with lower accuracy. Thus, it seems to be unlikely that the C–S bond densities are impaired by an accumulation of errors in the data of a particular group of reflections.

Dynamic and static experimental deformation densities

Here we give the deformation densities $\Delta\rho = \rho$(charge-cloud model) $- \rho$(free-atom model). Fig. 4 represents the dynamic densities, Fig. 5 the static densities (all vibration tensors put equal to zero). The static densities, particularly, are impaired by series termination and cannot be fully compared with theoretical densities. Obviously, thermal deconvolution pronounces the features; all bond peaks in Fig. 5 are higher, but the lone-pair peaks are not enhanced in agreement with the theoretical deformation density (see below, Fig. 6*a*).

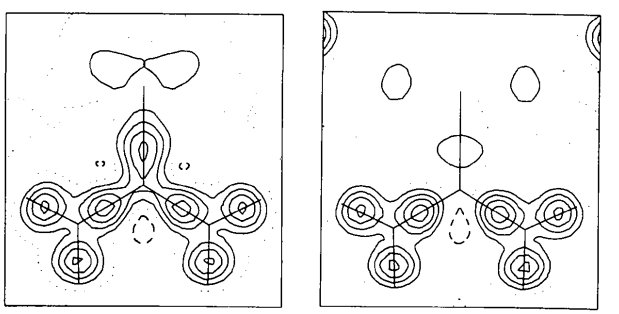

(*a*) (*b*)

Fig. 4. Dynamic deformation density as obtained from the charge-cloud model; otherwise as Fig. 1.

* A list of structure factors has been deposited with the British Library Lending Division as Supplementary Publication No. SUP 36438 (6 pp.). Copies may be obtained through The Executive Secretary, International Union of Crystallography, 5 Abbey Square, Chester CH1 2HU, England.

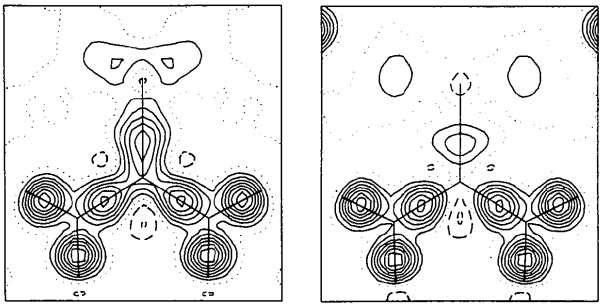

(*a*) (*b*)

Fig. 5. Static deformation density as obtained from the charge-cloud model; otherwise as Fig. 1.

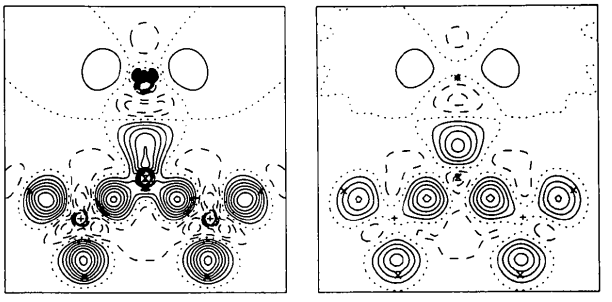

(*a*) (*b*)

Fig. 6. Theoretical (*a*) static and (*b*) dynamic deformation density. Contours are as in Fig. 1.

Comparison of the dynamic densities (Fig. 4) with the *X–X* maps (Fig. 2) shows a good agreement in general. The largest deviation is found behind the S atom in molecule (1): here, Fig. 2(*a*) displays a maximum of 0·22 e Å^{-3}, whereas Fig. 4(*a*) shows 0·10 e Å^{-3} in the corresponding position. In our model two separate charge clouds were used with (obviously) little overlap in the central region. Here the $F_o - F_c$ map also shows the largest residual of 0·19 e Å^{-3}. It is difficult to judge whether or not the uninterrupted distribution in the lone-pair region (Fig. 2*a*) represents the physical reality. The theoretical distribution (Fig. 6) shows separate maxima in the lone-pair region. With cyanuric acid, the *X–N* map shows a nearly uninterrupted lone-pair peak at one O atom, whereas at the other O atom two resolved peaks appear (Kutoglu & Scheringer, 1979).

Theoretical deformation densities

The AHF GTO (Approximate Hartree–Fock Gaussian-Type Orbital) wavefunction for the thiourea molecule (with a slightly idealized geometry of C_{2v} symmetry assumed) was calculated with the program *GAUSSIAN* 70 (Hehre, Lathan, Ditchfield, Newton & Pople, 1970) using the 4-31G (Ditchfield, Hehre & Pople, 1971) + BP (bond-polarization functions, Hase & Schweig, 1977) basis set. The BP's were localized at the middle of each bond; one *s* function with orbital exponent 1·0 for N–H, one *s* and a set of *p* functions with orbital exponents 1·55 and 0·65, respectively, for C–N and one *s* and a set of *p* functions with orbital exponents 0·6 and 0·5, respectively, for C–S (H. Meyer & A. Schweig, unpublished results). The atomic wavefunctions were calculated with the open-shell [Roothaan's (1960) open-shell procedure] part of the *POLYATOM* program system (Csizmadia, Harrison, Moskowitz & Sutcliffe, 1966) using the same basis set as for the molecule. Thermal smearing was performed with the method of Hase, Reitz & Schweig (1976) using the thermal parameters of Elcombe & Taylor (1968) for molecule (1) [note that the thermal parameters for molecule (2) are only insignificantly different from those of molecule (1) so that thermal smearing would lead to similar results in this case]. The calculated static and dynamic deformation densities are presented in Figs. 6(*a*) and 6(*b*), respectively.

Discussion

The agreement of the experimental densities with theoretical densities is now very satisfactory, particularly for molecule (1). For this molecule, the heights of the bond peaks in the *X–X* and theoretical deformation density maps agree within 0·04 e Å^{-3} and even the minima outside the molecule appear at the same positions. The deviation occurring in the lone-pair region (*i.e.* a rather extended peak in the *X–X* map) was discussed above. The minimum at the S atom is of less depth in the *X–X* map (Fig. 2*a*) and at 0·08 e Å^{-3} is no longer drawn; the theoretical density exhibits here a minimum of about −0·22 e Å^{-3}. Similarly, the dynamic density (Fig. 4*a*) and the theoretical density agree extremely well. Bond and lone-pair peaks deviate by at most 0·03 e Å^{-3}, except for the C–N peak where the theoretical peak is about 0·05 e Å^{-3} higher. Furthermore, in the experimental dynamic density, the level at the nuclear positions is higher, at N by 0·1 e Å^{-3} and at C by 0·4 e Å^{-3}, and the minimum at the S atom is missing. In general, experimental and theoretical deformation densities agree very well for molecule (1), as has rarely happened before for a molecular crystal.

The experimental deformation densities exhibit C–S bonding regions that are different for molecules (1) and (2). There are hints suggesting that this difference is not due to errors in the data or their treatment. These are the result of the Hamilton test on the R_w values and the fact that, according to the Fourier-transformation procedure of the experimental data, the same accuracy is to be expected for both molecules. At present, there are neither experimental nor theoretical arguments at hand to explain the differing C–S bond densities.

Whether or not there is a connection with the ferroelectric behaviour of thiourea below 169 K (Elcombe & Taylor, 1968) must be decided by future investigations.

Finally, for the quantum chemists it is gratifying to note that the present experimental reinvestigation was stimulated by the large deviations of the original experimental deformation densities from the corresponding theoretical densities. The present experimental reinvestigation has shown that errors in the original data had to be corrected and has then confirmed in detail the 4-31G + BP theoretical prediction. This is a further confirmation of the reliability and accuracy of theoretical deformation densities that are attainable on the economical level of 4-31G + BP AHF calculations.

This work was supported by the Deutsche Forschungsgemeinschaft, SFB Kristallstruktur und Chemische Bindung, Projekt H, and the Fonds der Chemischen Industrie. The quantum-chemical calculations were carried out on the TR 440 computer of the Rechenzentrum der Universität Marburg.

Note added in proof: In the process of publication we became aware of Mullen's (1982) paper (preceding paper). We believe that the differences in the deformation densities, as shown in the two papers, are due to the fact that Mullen used his old data in which the errors of the background measurements were not eliminated. In detail we make the following comments on the deformation densities.

(1) Mullen calculated only deformation densities (his Figs. 2, 3 and 6) which represent the difference of the multipole model and the free-atom model. Although, in principle, such deformation densities contain less irregular features (noise) than X–X(high-angle parameter) maps, Mullen's densities are more irregularly shaped than even our X–X map (Fig. 2) (in Mullen's Figs. 2, 3 and 6 there are a broad maximum at the N atom and large negative densities outside the molecule).

(2) The N—H bond peaks in Mullen's dynamic deformation densities appear to be too low (0·20–0·26 e Å^{-3}). Our N—H bond peaks (0·42–0·47 e Å^{-3}) agree fully with the peak heights of the theoretical calculation (Fig. 6*b* of our paper) and with those usually found in the literature [*e.g.* for cyanuric acid see Kutoglu & Scheringer (1979)].

(3) The agreement of the experimental and theoretical densities is better with our densities, the deviations being at most 0·05 e Å^{-3} for all peak heights (except for the C—S bond peak in molecule 2). With Mullen's bond peaks, the discrepancies in the theoretical dynamic density are about 0·16–0·22 e Å^{-3} for the N—H bonds, 0·10–0·14 e Å^{-3} for the C—S bonds, and 0·10 e Å^{-3} for the C—N bonds.

(4) Mullen's deformation densities of the two (half) molecules in the asymmetric unit look very similar because he constrained the density models for the two molecules to be the same. X–X(high-angle parameter) maps (our Figs. 1, 2 and 3), which do not depend on the particular model except for the phases, show that there are differences between the two molecules (in the C—S bonds) which become suppressed by the identical-density constraint.

References

CSIZMADIA, I. G., HARRISON, M. C., MOSKOWITZ, J. W. & SUTCLIFFE, B. T. (1966). *Theor. Chim. Acta*, **6**, 191–216; *Quantum Chemistry Program Exchange*, Indiana Univ. Program No. 199.

DIETRICH, H. & SCHERINGER, C. (1978). *Acta Cryst.* B**34**, 54–63.

DITCHFIELD, R., HEHRE, W. J. & POPLE, J. A. (1971). *J. Chem. Phys.* **54**, 724–728.

ELCOMBE, M. M. & TAYLOR, J. C. (1968). *Acta Cryst.* A**24**, 410–420.

FUESS, H., BATS, J. W., DANNÖHL, H., MEYER, H. & SCHWEIG, A. (1982). *Acta Cryst.* B**38**, 736–743.

HAMILTON, W. C. (1965). *Acta Cryst.* **18**, 502–510.

HASE, H. L., REITZ, H. & SCHWEIG, A. (1976). *Chem. Phys. Lett.* **39**, 157–159.

HASE, H. L. & SCHWEIG, A. (1977). *Angew. Chem.* **89**, 264–265; *Angew. Chem. Int. Ed. Engl.* **16**, 258–259.

HEHRE, W. J., LATHAN, W. A., DITCHFIELD, R., NEWTON, M. D. & POPLE, J. A. (1970). *Quantum Chemistry Program Exchange*, Indiana Univ. Program No. 236.

HIRSHFELD, F. L. (1976). *Acta Cryst.* A**32**, 239–244.

International Tables for X-ray Crystallography (1974). Vol. IV. Birmingham: Kynoch Press.

KUTOGLU, A. & SCHERINGER, C. (1979). *Acta Cryst.* A**35**, 458–462.

MULLEN, D. (1982). *Acta Cryst.* B**38**, 2620–2625.

MULLEN, D. & HELLNER, E. (1978). *Acta Cryst.* B**34**, 2789–2794.

MULLEN, D. & SCHERINGER, C. (1978). *Acta Cryst.* A**34**, 476–477.

REES, B. (1977). *Isr. J. Chem.* **16**, 180–186.

ROOTHAAN, C. C. J. (1960). *Rev. Mod. Phys.* **32**, 179–185.

SCHERINGER, C. (1980). *Acta Cryst.* A**36**, 205–210.